Sustainable activated carbons prepared from a sucrose-derived hydrochar: Remarkable adsorbents for pharmaceutical compounds

6 authors, including:

Ana Mestre
University of Lisbon
76 PUBLICATIONS   2,485 CITATIONS

SEE PROFILE

Marta Andrade
University of Lisbon
20 PUBLICATIONS   813 CITATIONS

SEE PROFILE

Margarida Galhetas
University of Lisbon
7 PUBLICATIONS   299 CITATIONS

SEE PROFILE

Cristina Freire
University of Porto Faculty of Sciences
362 PUBLICATIONS   10,444 CITATIONS

SEE PROFILE

Sustainable activated carbons prepared from a sucrose-derived hydrochar: remarkable adsorbents for pharmaceutical compounds†

Ana S. Mestre,*[ab] Emil Tyszko,[a] Marta A. Andrade,[a] Margarida Galhetas,[a] Cristina Freire[b] and Ana P. Carvalho*[a]

We present a two-step methodology for the preparation of highly activated carbons with tailored morphologies and micropore size distributions (MPSD) through the hydrothermal carbonization (HTC) of renewable biomass (*i.e.* sucrose) and further activation. Depending on the activation agent, activated carbons with spherical (K_2CO_3 or steam activation) or sponge-like morphologies (KOH activation) were obtained. The control of the activation variables allows tailoring the MPSD of the materials with K_2CO_3 activation at 700–800 °C originating porous materials with molecular sieve properties, and KOH activation giving porous carbon materials with wider MPSD. The highly developed porous structures of the activated carbons give them remarkable adsorption capacities for the removal of pharmaceutical compounds of distinct therapeutical classes (*i.e.* ibuprofen, paracetamol, clofibric acid, caffeine and iopamidol). Although the superactivated carbon obtained by the KOH activation at 800 °C has very high adsorption capacities for all the pharmaceutical compounds assayed, the material obtained by the K_2CO_3 activation at 800 °C has a similar adsorption capacity for all pharmaceuticals but iopamidol, the most voluminous compound. The distinct performance of the porous carbon materials for the removal of the pharmaceutical compounds is mainly related to their MPSD. The high performance of some of the synthetized carbons combined with the possibility of controlling the size of the particles in the HTC step allows not only their possible use as filter media but also coupling to other advanced water treatment technologies (*e.g.* membrane systems). Moreover, the abovementioned properties associated with the acidic surface chemistry of the developed activated carbons open new possibilities for the synthesis of functional carbon-based materials.

[a]*Centro de Química e Bioquímica, Faculdade de Ciências, Universidade de Lisboa, 1749-016 Lisboa, Portugal. E-mail: asmestre@fc.ul.pt; ana.carvalho@fc.ul.pt; Fax: +351 217500088; Tel: +351 217500897*

[b]*REQUIMTE/LAQV, Departamento de Química e Bioquímica, Faculdade de Ciências, Universidade do Porto, 4169-007, Portugal*

† Electronic supplementary information (ESI) available. See DOI: 10.1039/c4ra14495c

1. Introduction

The development of medical care and the use of increasingly more effective active pharmaceutical ingredients are unquestionably responsible for the high lifestyle standards of modern society. However, the large consumption of pharmaceuticals possess a great stress to the aquatic environment because these compounds are not totally removed/degraded by the implemented water treatment technologies, leading to toxic effects in aquatic organisms.[1,2] This reality led to a widespread consensus between scientists and governmental entities, which consider that this type of contamination may require legislative intervention, with various pharmaceuticals appearing in a Watch List in the 2013/39/EU directive. The recalcitrant behavior of pharmaceutical compounds in conventional water treatment plants requires the use of more powerful treatment processes to ensure the maintenance of water quality. Adsorption by activated carbons arises as one of the best available technologies to face this threat,[3] mainly due to its non-specific adsorption properties.

Hydrothermal carbonization (HTC) is a cost effective and eco-friendly process to obtain spherical hydrophilic materials from carbon rich precursors (including renewable carbohydrate-rich biomass); it uses water as solvent, mild temperatures and self-generated pressure with no CO_2 emission. Carbon materials obtained from HTC, hydrochars, have outstanding properties related to their spherical morphology and high content of oxygenated surface groups, which can be used for the synthesis of functional carbon-based materials.

The potentialities of hydrothermal carbons, including their use as precursors for the preparation of porous and/or functional materials and for the synthesis of nanocomposites, were recently reviewed by Titirici *et al.*[4] Therefore, in the last few years, carbon materials obtained by HTC have been used in the challenging areas of the modern society such as catalysis,

energy storage, CO_2 sequestration or water purification.[4,5] However, in adsorption processes, hydrochars have as major drawbacks low porosity and surface area. Several activation routes have been assayed to increase their textural properties,[6–10] although the most commonly used activation methodology employing KOH generally promotes the disruption of the spherical morphology of the resulting activated carbon materials. In a newly published work by our group, it was proved that sucrose-derived hydrochars activated with K_2CO_3 are high performance materials for methane storage or biogas upgrade, mainly due to the combination of narrow micropore size distributions and microspherical morphology that leads to high packing density, only attained with K_2CO_3 activation.[10]

Considering the promising results from our previous publication, the first aim of the present work was to evaluate the effect of activating agent, impregnation methodology and activation temperature in the textural and morphological characteristics of hydrochar-derived activated carbons. The preparation procedure is a two-step route involving an initial hydrothermal treatment of sucrose followed by physical (steam) or chemical (KOH and K_2CO_3) activation. The second aim of this work was to evaluate the potentialities of these eco-friendly activated carbons for the adsorption of several pharmaceutical compounds from distinct therapeutic classes (*i.e.* ibuprofen, paracetamol, clofibric acid, caffeine and iopamidol). The highly developed microporous structure and tunable porosity of these sucrose-derived materials revealed to be crucial for their remarkable adsorption capacities for pharmaceutical compounds with very distinct chemical moieties and dimensions, when compared with activated carbons prepared from lignocellulosic materials by conventional activation processes, or even with commercial carbons used in conventional water treatment technologies.[11–19]

2. Experimental section

2.1 Chemical compounds

All chemicals were used as received: sucrose (Analar Normapur, >90%), potassium carbonate (Aldrich, 99%), potassium hydroxide (Panreac, 85%), ibuprofen (Sigma-Aldrich – Lot BCBC9914V), paracetamol (Merck – Lot S6137725 035, ≥99%), caffeine (Normapur – Batch 08J300011, analytical grade), clofibric acid (Alfa Aesar – Lot G1266B, 98%) and iopamidol (synthesized by Hovione – Lot 163926HQ01324).

2.2 Activated carbons synthesis

The sucrose-derived activated carbons were prepared by two consecutive steps:[10] a hydrothermal carbonization of a sucrose solution followed by a chemical or physical activation of the hydrochar.

The hydrochar was synthetized introducing 15 cm^3 of a 1.5 mol dm^{-3} sucrose aqueous solution in a Teflon-line stainless steel autoclave. The HTC was generated during 5 h at 190 °C in an oven (Medline Scientific Limited, model ON-02G) pre-heated to the desired temperature. The autoclave was cooled down to room temperature, and the powder (hydrochar S) was further washed with distilled water and acetone and dried (60 °C).

For steam activation, the hydrochar (1 g) was introduced in a quartz reactor placed in a vertical furnace (Thermolyne, model 21100). The steam was generated in a bubbler with distilled water at 90 °C and carried by a N_2 flow (8 cm^3 s^{-1}). The material was activated at 800 °C during 1 h (10 °C min^{-1}); subsequently, the steam flow was turned off and the material was cooled to room temperature under N_2.

For chemical activation, 1 g of hydrochar was impregnated in a solution with 4 g of K_2CO_3 or KOH during 2 h and then dried; for K_2CO_3, a physical impregnation was also used. Activation was performed at temperatures between 600 and 900 °C in a horizontal furnace (Thermolyne, model 21100) for 1 h under a N_2 flow of 5 cm^3 s^{-1} (10 °C min^{-1}). After cooling under a N_2 flow, the materials were thoroughly washed with distilled water until pH 7 was reached, dried overnight at 100 °C and stored. The materials are labelled as S (hydrochar) followed by the activating agent abbreviation (St, H and C for steam, KOH and K_2CO_3, respectively) and the temperature (°C). Materials prepared by physical impregnation are labelled with a P (physical) after the activation temperature.

For comparison purposes, commercial carbons used in water remediation processes were also tested (CP and VP materials supplied by Quimitejo, Portugal, and NS material supplied by Norit, Salmon & Cia, Portugal).

2.3 Characterization of the activated carbons

The textural properties of the activated carbons were characterized by N_2 adsorption isotherms obtained in an automatic equipment (Micromeritics ASAP 2010) at −196 °C and by CO_2 adsorption isotherms acquired in a conventional volumetric apparatus equipped with a MKS-Baratron (310BHS-1000) pressure transducer (0–133 kPa). Before the isotherms acquisition, the solid materials (∼50 mg) were outgassed overnight at 120 °C under vacuum (pressure < 10^{-2} Pa). The N_2 isotherms were used to estimate the apparent specific surface area, A_{BET}, applying the BET equation in the range $0.05 < p/p^0 < 0.15$,[20] and also the total pore volume, V_{total}, using the Gurvich rule,[21] corresponding to the volume of N_2 adsorbed at $p/p^0 = 0.975$. The microporosity was assessed applying the Dubinin–Radushkevich (DR) equation to the N_2 and CO_2 adsorption data ($W_{0\ N_2}$ and $W_{0\ CO_2}$, respectively). The α_S method was also applied to the N_2 adsorption data, taking as reference the isotherm reported by Rodríguez-Reinoso *et al.*[22] With this method, the values of total micropore volume, $V_{\alpha\ total}$, ultramicropore volume (width less than 0.7 nm), $V_{\alpha\ ultra}$, and supermicropore volume (width between 0.7 and 2 nm), $V_{\alpha\ super}$, were obtained.[20] The mesoporous volume, V_{meso}, corresponds to the difference between V_{total} and $V_{\alpha\ total}$. The micropore size distributions were obtained from the CO_2 adsorption isotherms, according to the method described by Pinto *et al.*[23]

The surface chemistry of the materials was characterized by the determination of the pH at the point of zero charge (pH_{PZC}), following the reversed mass titration procedure.[15,24] Briefly, a slurry of 10% was prepared by mixing the activated carbon with ultra-pure water in a glass bottle, bubbled and sealed under N_2 (to eliminate CO_2). The pH of the slurry was measured

(Symphony SP70P pH meter) after shaking it for at least 24 h at room temperature. In order to obtain the pH values for lower solid weight fractions, this procedure was repeated for slurries of 8%, 6%, 4%, 2% and 1% obtained by the successive dilutions of the initial 10% slurry. The pH_{PZC} value corresponds to the plateau of the curve of equilibrium pH *versus* solid weight fraction. The analysis of the elemental composition was performed using an Elemental Analyser (EA 1108 CHN-O Fisions Instruments) at "Laboratório de Análises", IST, Lisboa (Portugal). Finally, the morphological characterization of the hydrochar (S) and the activated carbons was performed by scanning electron microscopy (SEM, JEOL, mod. 7001F) using an accelerating voltage of 25 kV.

2.4　Liquid phase adsorption

The sucrose-derived activated carbons and three commercial materials were tested as adsorbents of pharmaceutical active compounds (PhACs) through three sequential types of assays: screening, kinetic and equilibrium. As target molecules, five PhACs were selected: ibuprofen, paracetamol, caffeine, clofibric acid and iopamidol. The pharmaceutical compound solutions were prepared with ultra-pure water obtained from Milli-Q purification systems, and no pH adjustments were made. With the exception of the clofibric acid and caffeine solutions, which have a pH value of ∼3 and ∼7, respectively, all the other solutions presented pH values around 5.

In a typical experiment, a known amount of activated carbon and PhAC solution were mixed in a glass flask that was introduced in a water bath at 30 °C (Grant GD100 controller) and stirred at 700 rpm (multipoint agitation plate Variomag Poly), being the sample collected after the desired contact time (see details in Table 1). After filtration, the remaining amount of PhAC was determined by UV-vis spectrophotometry (Genesys 10S) at the wavelength corresponding to the maximum of absorbance: 221 nm (ibuprofen), 243 nm (paracetamol), 228 nm (clofibric acid), 272 nm (caffeine), and 242 nm (iopamidol). PhAC uptake was calculated according to the following equation:

$$q_t = \frac{C_0 - C_t}{W} \times V \tag{1}$$

where q_t is the amount (mg g^{-1}) of PhAC adsorbed at time t, C_0 is the PhAC initial concentration (mg dm^{-3}), C_t is the PhAC concentration at time t (mg dm^{-3}), V is the volume (dm^3) of the PhAC solution and W is the weight (g) of dried carbon.

The screening, kinetics and equilibrium assays were carried out according to the experimental conditions summarized in Table 1. All the kinetic and equilibrium adsorption assays were made in triplicate. The results from the preliminary screening assays allowed to evaluate the removal efficiencies (removal efficiency = $[(C_0 - C_{24\,h})/C_0] \times 100$, where C_0 and $C_{24\,h}$ are the initial concentration of PhAC and that determined after 24 h in contact with activated carbon, respectively). The kinetic data were analysed considering the pseudo-first and pseudo-second order kinetic models,[25] whereas the equilibrium adsorption data were analysed considering linear forms of the Langmuir[26] and Freundlich[27] isotherm models presented in Table S1 of ESI.†

Table 1 Experimental conditions used in the screening, kinetic and equilibrium assays. The activated carbons tested and pharmaceutical active compounds (PhACs) used as target molecules for each assay are also presented

Assay	Activated carbons	PhAC	Conditions
Screening	SH800 SH700 SC800 SC800P CP VP NS	Ibuprofen Paracetamol Caffeine Clofibric acid Iopamidol	$m_{AC} = 6$ mg $V_{PhAC} = 9$ and 30 cm^3 [PhAC] $= 180$ mg dm^{-3} $t_{contact} = 24$ h
Kinetic	SH800 SC800 NS	Paracetamol Iopamidol	$m_{AC} = 6$ mg $V_{PhAC} = 30$ cm^3 [PhAC] $= 180$ mg dm^{-3} $t_{contact} = 1$ min to 48 h
Equilibrium	SH800 SC800 NS	Paracetamol Iopamidol	$m_{AC} = 6$ mg $V_{PhAC} = 9$ and 30 cm^3 [PhAC] $= 45$–300 mg dm^{-3} $t_{contact} = 24$ h

3.　Results and discussion

3.1　Activated carbons properties

The morphological analysis performed by SEM (Fig. 1) reveals that the sucrose-derived hydrochar S is constituted by spheres with diameters of around 3 μm. The solids activated with steam (SSt800) and K_2CO_3 (SC800 and SC800P) at 800 °C retain the spherical morphology and smooth surface of the pristine hydrochar, whereas K_2CO_3 activation at 900 °C (SC900) originates microspheres with a rough (exfoliated) surface. On the contrary, the use of KOH as activating agent (materials SH600, SH700 and SH800) promoted the disruption of the spherical morphology, regardless of the activation temperature used. In fact, in the range of activation temperatures studied (600–800 °C), KOH-activated materials have always a sponge-like morphology (Fig. S1 of ESI†), and the lower the activation temperature, the smaller the amount of cavities present in the smooth surface.

The N_2 isotherms of the materials activated at 800 °C (Fig. 2) reveal that different activation agents and procedures originated porous materials with well developed microporosity (type I isotherms). KOH activation produced the material with the most developed microporous structure, but at the expense of the spherical morphology (Fig. 1). The activation with K_2CO_3 originated microspheres with significantly lower adsorption capacities, and the spherical material obtained by steam activation has the less developed microporous network. The effect of the impregnation methodology in the activation with K_2CO_3 is illustrated by materials SC800 (solution) and SC800P (physically) with the wet impregnation allowing a higher development of the microporous structure, as expected. From all the isotherms presented in Fig. 2, carbon SH800 has a rounder off knee, which is a characteristic of the widening of the micropore size distribution due to the formation of larger micropores (supermicropores).
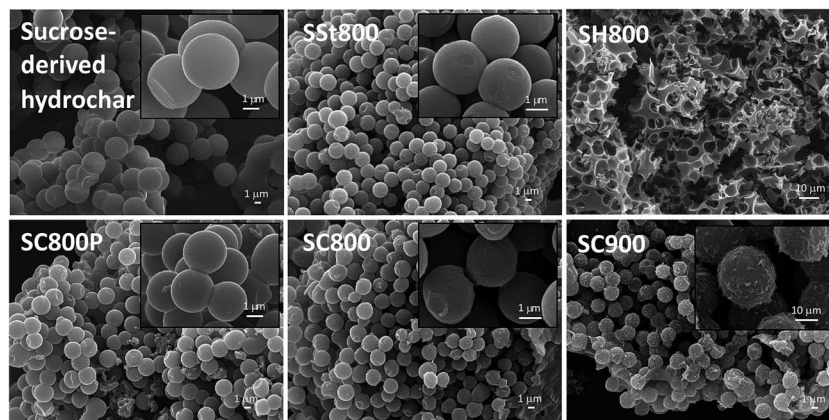
Fig. 1 SEM images of sucrose-derived hydrochar and activated carbons. The insets correspond to higher amplifications to better illustrate the surface of the materials.
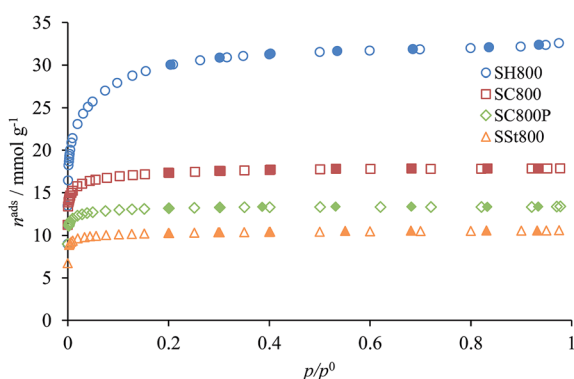

Fig. 2 N$_2$ adsorption–desorption isotherms at −196 °C of the sucrose-derived carbons activated with KOH (SH800), K$_2$CO$_3$ (SC800 and SC800P) and steam (SSt800) at 800 °C. Closed symbols are desorption points.

The textural parameters of the activated carbons (Table 2) reveal that although the KOH activation leads to a higher porosity development ($A_{BET} \sim 2500$ m^2 g^{-1}), the use of K$_2$CO$_3$ allowed a better compromise between the porosity development ($A_{BET} \sim 1400$ m^2 g^{-1}) and the yield of the activation process (45% *vs.* 13% for materials SC800 and SH800, respectively). The impregnation methodology also influenced the textural parameters: impregnation in solution originates solids with 32% to 42% higher micropore volumes than those obtained by physical impregnation, but the yields of the two procedures were very similar.

The analysis of the microporosity assessed from the α_s method and the DR equation applied to N$_2$ and CO$_2$ adsorption data reveal that the materials have distinct microporous structures. Materials activated with KOH at 700 and 800 °C have higher micropore volumes assessed by N$_2$ data ($W_{DR\ N_2}$) and higher volumes of larger micropores ($V_{\alpha\ super}$), whereas the materials activated at the same temperatures but with K$_2$CO$_3$ have higher volumes assessed by CO$_2$ data ($W_{DR\ CO_2}$), which is in agreement with the higher volumes of narrow micropores assessed by N$_2$ data ($V_{\alpha\ ultra}$), given in Table 2. Concerning the

activation with K$_2$CO$_3$, it is interesting to notice that the activation at 900 °C, which originated microspheres with rougher surface, leads to a porous material with a higher predominance of supermicropores ($V_{\alpha\ super}$) and also with a mesopore volume that corresponds to 14% of the total pore volume, whereas all the other K$_2$CO$_3$-activated materials obtained at lower temperatures are exclusively microporous solids. It is worth noting that the preparation yield of this material (SC900) is only slightly lower than those of the materials prepared at lower temperatures.

Further characterization of the carbons' microporous structure by micropore size distributions (MPSDs) assessed from CO$_2$ data (Fig. 3) reveals that regardless of the chemical activating agent (Fig. 3(a) and (b)), the increase of the activation temperature leads to the broadening of the micropore size distribution, changing from a monomodal to a bimodal distribution. Materials SC700P, SC800P and SC700 (Fig. 3(b) and (c)) present very narrow micropore size distributions, centred at 0.52 nm for SC700P and at 0.61 nm for the other two materials, pointing out that the lower the porosity development (Table 2), the smaller the micropore width of the material. Comparing the MPSDs of the sucrose-derived carbons with those of the carbons commercialized for water treatment, it is clearly seen that the majority of the lab-made materials present considerably higher volumes of narrow micropores, which, in the particular case of materials SH700 and SH800, are also associated to high volumes of larger micropores. In fact, the superactivated carbon SH800 combines high volumes of micropores with widths between 0.6 and 1.0 nm with micropores larger than 1.3 nm. The volume of the latter is more than two times higher than those of commercial materials CP or NS (Fig. 3(a) and (d)).

In conclusion, using K$_2$CO$_3$ as activating agent in optimized conditions, the methodology followed allowed the preparation of microspherical activated carbons with high micropore volumes and very narrow micropore size distributions centred at widths <0.7 nm, thus showing molecular sieve properties. On the other hand, the activation of the sucrose-derived hydrochar with KOH leads to materials with very high micropore volumes, and with textural parameters and preparation yields in

Table 2 Textural properties of the activated carbons, preparation yield (η, defined as g of activated carbon per 100 g of hydrochar), maintenance or no maintenance of the hydrochar spherical shape, and pH$_{PZC}$ value

| Materials | η (%) | Spherical shape | A_{BET} (m^2 g^{-1}) | $V_{total}{}^a$ (cm^3 g^{-1}) | $V_{meso}{}^b$ (cm^3 g^{-1}) | α_s method | | | DR equation | | pH$_{PZC}$ |
						$V_{\alpha\ total}$ (cm^3 g^{-1})	$V_{\alpha\ ultra}$ (cm^3 g^{-1})	$V_{\alpha\ super}$ (cm^3 g^{-1})	$W_{DR\ N_2}$ (cm^3 g^{-1})	$W_{DR\ CO_2}$ (cm^3 g^{-1})	
Steam											
SSt800	38	Yes	814	0.37	0.01	0.36	0.25	0.11	0.36	0.45	8.6
KOH											
SH600	25	No	1169	0.57	0.07	0.50	0.17	0.33	0.49	0.50	—
SH700	24	No	1987	0.91	0.05	0.86	0.16	0.71	0.79	0.71	—
SH800^c	13	No	2431	1.14	0.06	1.08	0.00	1.08	0.90	0.71	4.0
K$_2$CO$_3$											
SC700	55	Yes	987	0.44	0.00	0.44	0.33	0.11	0.43	0.57	—
SC700P^c	51	Yes	694	0.31	0.00	0.31	0.23	0.08	0.31	0.41	—
SC800^c	45	Yes	1375	0.63	0.01	0.62	0.35	0.27	0.58	0.65	4.3
SC800P	48	Yes	1053	0.47	0.00	0.47	0.30	0.17	0.46	0.52	4.9
SC900	40	Yes	1200	0.59	0.08	0.51	0.21	0.30	0.50	0.50	—
Commercial											
CP	—	No	907	0.43	0.03	0.40	0.16	0.24	0.40	0.27	10.3
VP	—	No	758	0.43	0.13	0.30	0.15	0.15	0.32	0.29	9.8
NS	—	No	1065	0.70	0.30	0.40	0.02	0.38	0.39	0.27	8.4

^{a} Evaluated at $p/p^0 = 0.975$ in the N$_2$ adsorption isotherms at $-196\ ^{\circ}$C. ^{b} Difference between V_{total} and $V_{\alpha\ total}$. ^{c} Data from ref. 10.

accordance with those reported in previous studies concerning activated carbons obtained by the KOH activation of hydrochars prepared from carbohydrates or biomass in similar experimental conditions.[6–8] The loss of the hydrochar spherical morphology after the KOH-activation, herein observed regardless of the temperature used, was also reported previously.[8,28] It is commonly accepted that the activation with KOH and K$_2$CO$_3$ will incorporate metallic potassium in the carbon structure during activation, and its removal during the washing step will be responsible for unblocking the micropore network.
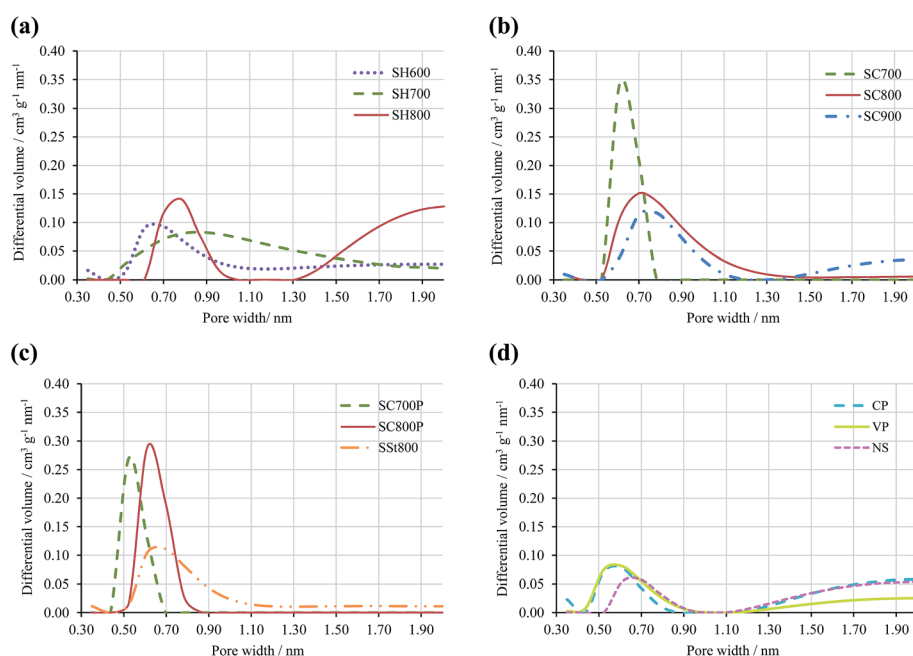

Fig. 3 Micropore size distributions obtained by fitting the CO$_2$ adsorption isotherms at 0 $^{\circ}$C to the method described by Pinto et al.[23] (a) Sucrose-derived carbons activated with KOH; (b) sucrose-derived activated carbons impregnated in solution with K$_2$CO$_3$; (c) sucrose-derived activated carbons physically impregnated with K$_2$CO$_3$ and sucrose-derived carbon activated with steam; (d) commercial materials.

Therefore, the fact that KOH and K_2CO_3 activation lead to the synthesis of carbons with sponge-like morphology and spherical activated carbons, respectively, was earlier interpreted as an indicative of the fact that the activation with these chemicals follows distinct mechanisms.[10] In fact, the KOH activation mechanism involves reactions that start at $\sim$400 °C, leading to the formation of several gases that, in addition to the presence of K compounds, can also contribute to the activation of the precursor.[29–31] On the other hand, K_2CO_3, which is also formed during the KOH activation mechanism, decomposes only at 700–800 °C,[29–31] leading to a less extensive consumption of the carbon matrix and consequently allowing the spherical morphology of the hydrochar to be retained after the activation.

It is interesting to notice that the spherical morphology of the K_2CO_3-activated materials lead to considerably higher densities (tap and packing) when compared with the KOH-activated carbon SH800.[10] This property is crucial for the application of these materials in storage vessels of separation processes because an activated carbon with a high packing density allows the use of smaller storage containers or separation towers.

Concerning the surface chemistry, the pH_{PZC} values (Table 2) of the materials activated at 800 °C reveal that the steam activation produces a material with basic surface chemistry (pH_{PZC} 8.6), whereas the chemical activation produces acidic carbons (pH_{PZC} 4.0 and 4.9) but less acidic than the hydrochar (pH_{PZC} 2.1). The elemental analysis data indicate that material SH800 is the one presenting the lower percentage of carbon (74.5 wt%), the material activated with steam, SSt800, has the highest carbon percentage (87.1 wt%) and the K_2CO_3-activated material, SC800, has 81.2 wt% of carbon. Amounts of other heteroatoms were similar for these three materials, and below 0.5% for nitrogen and 2% for hydrogen and sulfur. The elemental compositions of the sucrose-derived activated carbons are in the usual range of values obtained for activated carbon materials prepared from hydrochars, other precursors and also commercial materials.[7,12,17,32]

The commercial activated carbons used for comparison purposes are micro and mesoporous materials with the exception of the material CP, which is only microporous (Table 2). Although carbon NS has mainly supermicropores, the other commercial samples present both ultra and supermicropores. The pH_{PZC} values of the commercial carbons range between 8.4 and 10.3, which is indicative of materials with basic surface chemistry.

3.2 Liquid phase adsorption

Although the highly microporous carbons obtained by activation of hydrochars have been tested mainly in energy storage applications,[4,7,9,10,28,33,34] their well-developed micropore network, surface chemistry and morphology turn them into very interesting materials also for liquid phase applications. In this study, the sucrose-derived activated carbons were, to the best of our knowledge, tested for the first time as adsorbents for the removal of several pharmaceutical compounds in liquid phase: ibuprofen and paracetamol (analgesics), clofibric acid

(metabolite of lipid regulators), caffeine (stimulant) and iopamidol (iodinated contrast medium). The molecular structure, solubility, pK_a, log K_{ow} and the dimensions of the above-mentioned pharmaceuticals are summarized in Table 3.
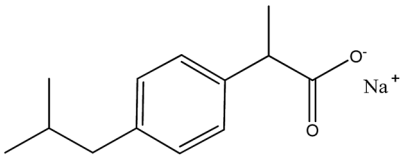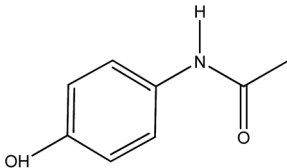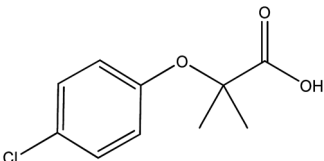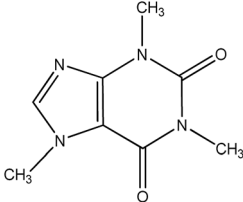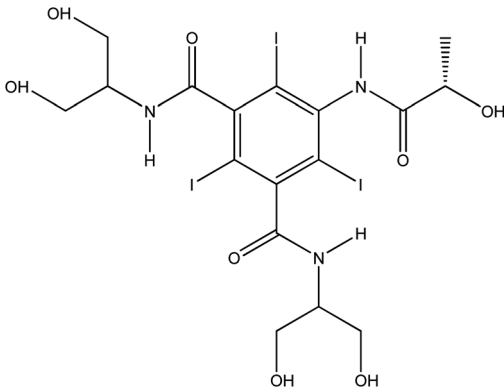
The data gathered reveal that the target pharmaceutical compounds of this study have different hydrophilic–hydrophobic characters (water solubility and log K_{ow} values); on the other hand, some of them are present in solution as aggregates. If fact, previously reported data reveal that in the experimental conditions used in the present work (pH $\sim$ 5), paracetamol can be present in solution as a monomer or dimer,[35] whereas iopamidol may be in the form of a monomer, dimer or trimer,[18] which leads to species with very distinct dimensions in solution.[18]

With the exception of ibuprofen, which was used in the form of sodium salt, for all the other pharmaceuticals, the log–log octanol–water partition coefficient (K_{ow}) and water solubility (S_w) are linear related (see Fig. S2 of ESI†), which is in accordance with larger sets of data concerning organic compounds.[36,37] According to the hydrophilic–hydrophobic characteristics, and excluding ibuprofen, which is an anion, the PhACs can be ordered from the most hydrophilic to the most hydrophobic as iopamidol, caffeine, paracetamol and clofibric acid.

3.2.1 Screening studies of PhACs removal. The performance of selected lab-made materials and activated carbons commercialized for water treatment technologies for the removal of pharmaceutical compounds was made throughout the evaluation of the removal efficiencies. For illustration purposes, the removal efficiencies achieved by the tested activated carbons for clofibric acid are displayed in Fig. 4. The lab-made carbons prepared by chemical activation of the hydrochar outperformed the commercial materials, attaining removal efficiencies near 100% (bars above the orange horizontal line that marks the removal efficiency attained with the best commercial carbon – material NS). Fig. S3 of ESI† resumes the removal efficiencies attained for all the systems, and it is interesting to notice that each particular carbon presents similar removal efficiencies for paracetamol, clofibric acid and caffeine. Ibuprofen and iopamidol were the compounds for which more distinct removal efficiencies were attained. Ibuprofen is systematically less removed than all the other small PhACs, which is certainly related with its ionic character that is associated to a high solubility in water. Concerning iopamidol, the most voluminous compound, with exception of the lab-made materials SH800 and SH700, all the other activated carbons present removal efficiencies considerably lower (<50%) than those obtained for the other molecular PhACs (>50%).

Fig. 5 presents the removal efficiency variation of each carbon against the best commercial material assayed for each pharmaceutical compound, i.e. carbon NS. It is clearly seen that the lab-made carbons SH800 and SH700, prepared by the KOH activation of the hydrochar, attain removal efficiencies at least 10 percentage points higher than the NS material. In the case of the most voluminous molecule, iopamidol, the removal efficiency of these carbons is almost the double of that obtained with carbon NS. The very high removal efficiencies of materials

Table 3 Molecular structure, solubility in water (S_w), pK_a, log K_{ow} and the dimensions of the pharmaceutical compounds under study. The critical dimension of each specie is highlighted in bold

Pharmaceutical compound	Molecular structure and other relevant properties	
Ibuprofen (Ibu)	1.32 (length) × **0.72** (width) × 0.77 (thickness) in nm (ref. 17)	log K_{ow} = 4.0 (ref. 38) S_w = 100 000 mg dm^{-3}
Paracetamol (Para)	Monomer – 1.19 (length) × 0.75 (width) × **0.46** (thickness) in nm (ref. 11) Dimer – 1.58 (length) × 1.19 (width) × **0.66** (thickness) in nm (ref. 11)	log K_{ow} = 0.46 (ref. 39) S_w = 17 390 mg dm^{-3} (ref. 40) pK_a = 9.7 (ref. 41)
Clofibric acid (Clof)	1.22 (length) × **0.70** (width) × 0.72 (thickness) in nm (ref. 42)	log K_{ow} = 2.57 (ref. 38) S_w = 755 mg dm^{-3} (ref. 17) pK_a = 2.9
Caffeine (Caf)	1.06 (length) × 0.85 (width) × **0.45** (thickness) in nm (ref. 19)	log K_{ow} = −0.5 (ref. 39) S_w = 30 000 mg dm^{-3} (ref. 13)
Iopamidol (Iop)	Monomer – 1.5 (length) × 1.5 (width) × **0.6** (thickness) in nm (ref. 18) Dimer – 1.5 (length) × 1.5 (width) × **1.2** (thickness) in nm (ref. 18) Trimer – 1.5 (length) × **1.5** (width) × 1.8 (thickness) in nm (ref. 18)	log K_{ow} = −2.42 (ref. 38) S_w > 200 000 mg dm^{-3} (ref. 43) pK_a = 10.7

SH800 and SH700 for this particular PhAC is certainly related to their micropore size distributions, because the large amount of wider micropores allows the adsorption of all the iopamidol species (monomers, dimers and trimers).

The lab-made carbons SC800 and SC800P also present very high removal efficiencies for the small PhACs (in the case of material SC800, comparable to those of materials activated with KOH), but are less effective for the removal of iopamidol, certainly due to their narrower micropore size distributions, centered at width ∼0.7 nm (Fig. 3(b) and (c)). Contrary of what occurs for KOH-activated materials, the micropore network of carbon SC800P only allows the adsorption of the iopamidol monomer, and material SC800, although presenting a broader micropore size distribution, may adsorb monomers and
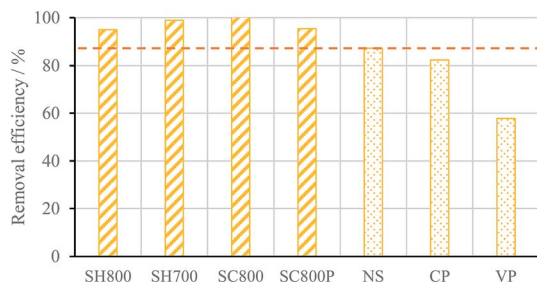
Fig. 4 Removal efficiency of the mentioned activated carbons for clofibric acid (6 mg carbon/9 cm^3 solution with 180 mg dm^{-3}, 24 h contact time at 30 °C). The orange horizontal line marks the removal efficiency attained with the best commercial carbon (NS).

dimers, but does not present pores that can accommodate the iopamidol trimer (*i.e.* micropores with width >1.5 nm).

The screening results reveal the potentialities of the hydrochar-derived activated carbons for the removal of pharmaceutical compounds of distinct therapeutical classes and with different chemical properties. In general, the characteristics of the carbons' micropore network correlate well with the removal efficiencies attained for the several PhACs, considering their critical dimensions.

In order to get more insights into the adsorptive properties of the lab-made materials, two pharmaceutical compounds were selected: paracetamol, which is an over-the-counter medicine, and iopamidol, a contrast media and the bulkiest compound under study.

The screening assays using larger amounts of paracetamol or iopamidol for the same dose of adsorbent, Fig. S4 of ESI,† corroborate the trends observed in Fig. 5 and highlight the superior adsorption performance of the majority of

the chemically activated lab-made carbons for both pharmaceuticals.

3.2.2 Paracetamol and iopamidol kinetic adsorption studies. In order to have a deeper evaluation of the adsorptive properties of the sucrose-derived activated carbons and considering the preliminary results obtained in the screening assays, kinetic and equilibrium adsorption studies were made for the chemically activated materials SH800 and SC800 and also for the best performing commercial carbon (NS).

The kinetic curves for both pharmaceuticals are presented in Fig. 6 showing that in all the cases, the paracetamol adsorption equilibrium is reached in about 1 h of contact time, and that lab-made materials have similar kinetic profiles, but attained higher removal efficiencies than the commercial material. Concerning iopamidol, very distinct kinetic profiles are observed for the tested carbons.

The experimental data were fitted to the pseudo-first[44] and pseudo-second[25] order kinetic models and presented a best fitting to the pseudo-second order kinetic model for both compounds. The correspondent kinetic parameters are quoted in Table 4. For paracetamol, the initial adsorption rate (h) is in the same order of magnitude for all the carbons, whereas in the
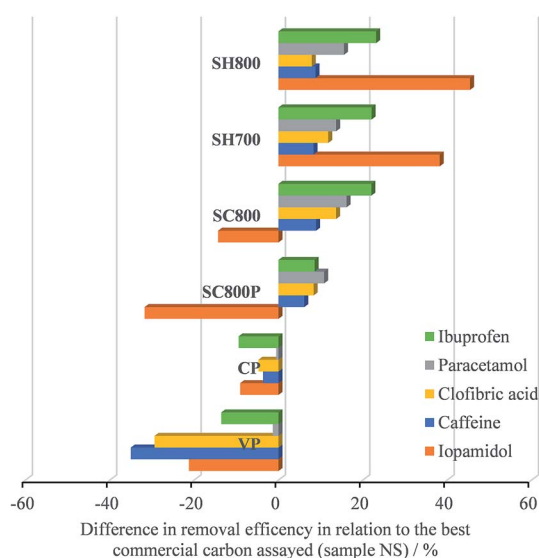

Fig. 5 Removal efficiency variation of each carbon against the best commercial material assayed (NS) for the mentioned pharmaceutical compounds (6 mg carbon/9 cm^3 of PhAC solution with 180 mg dm^{-3}, 24 h of contact time at 30 °C).
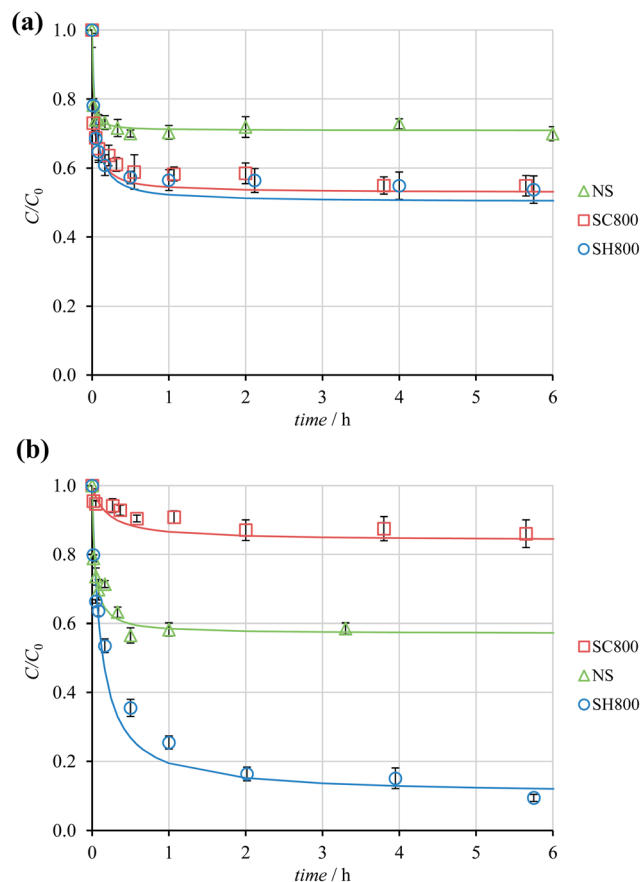

Fig. 6 Kinetic results of paracetamol (a) and iopamidol (b) adsorption onto the mentioned carbons at 30 °C. Symbols correspond to the experimental data, whereas lines represent the fitting to the pseudo-second-order kinetic equation (6 mg carbon/30 cm^3 of PhAC solution with 180 mg dm^{-3}). Error bars are included.

Table 4 Pseudo-second order PhACs adsorption parameters for the studied carbon materials at 30 °C: k_2 is the pseudo-second order rate constant; h is the initial adsorption rate; $t_{1/2}$ is the half-life time; $q_{e,calc}$ and $C_{e,calc}$ are the PhAC uptake and that remaining in solution at equilibrium, respectively, both calculated by the pseudo-second order kinetic model. RE is the removal efficiency (RE = $((C_0 - C_e)/C_0) \times 100$)

Material	k_2 (g mg^{-1} h^{-1})	R^2	h (mg g^{-1} h^{-1})	$t_{1/2}$ (h)	$q_{e,calc}$ (mg g^{-1})	$C_{e,calc}$ (mg dm^{-3})	RE (%)
Paracetamol							
SH800	0.050	0.999	10 000	0.045	448.4	90.3	49.8
SC800	0.070	0.999	12 500	0.034	423.7	95.3	47.1
NS	0.292	0.997	20 000	0.013	261.8	127.6	29.1
Iopamidol							
SH800	0.011	0.999	7143	0.113	806.5	18.7	89.6
SC800	0.036	0.990	735	0.196	143.9	151.2	16.0
NS	0.075	0.999	11 111	0.035	386.1	102.8	42.9

case of iopamidol, distinct orders of magnitude are observed, and the materials can be ordered as NS > SH800 ≫ SC800.

The higher initial iopamidol adsorption rate of NS is related to its high volume of mesopores, which allows a fast diffusion of this voluminous compound, in accordance with previously reported data.[18] However, considering that the removal efficiency of iopamidol ranges from 16.0% to 89.6%, a more accurate evaluation of the overall kinetic process should be made through the global adsorption rate (k_2). These values reveal a considerably faster global adsorption rate for the lab-made materials and particularly for carbon SH800.

The initial and global adsorption rates (h and k_2, respectively) of paracetamol by the lab-made materials SC800 and SH800 are very similar, although these materials present very distinct volumes of micropores. Their similar adsorption rates can be tentatively related to their micropore size distributions, because both carbons have very high volume of micropores with widths higher than the critical dimensions of the paracetamol species (0.46 and 0.66 nm) compared with the commercial carbon NS, which allows a faster diffusion towards adsorption sites.

Although the mesopore volume controls the rate of the initial iopamidol adsorption process, the removal efficiency (RE) is linearly related with $V_{\alpha\ super} + V_{meso}$ (determination coefficient of 0.987, Fig. S5 of ESI†). This finding is in accordance with the results obtained in a previous study using other commercial and lab-made materials,[18] where the paramount importance of the carbons' micropore size distributions for the adsorption of iopamidol, which may be present in the form of monomers (0.6 nm), dimers (1.2 nm), trimers or bigger aggregates (1.5 nm) was proved. Although the micropore size distributions of the best performing carbon, SH800, and the commercial material NS allow to conclude that all iopamidol species can be adsorbed, the micropore size distribution of material SC800 indicates that only the monomer and dimer forms can access the adsorption sites. However, from the conductivity data of aqueous iopamidol solutions,[18] we can assume that in the range of concentrations used, and particularly for the concentration of iopamidol remaining in solution at equilibrium when SC800 was used (i.e. 151.2 mg dm^{-3}), iopamidol will be present as a trimer or bigger aggregate. This justifies the lowest removal efficiency attained

with SC800 and the better performance of the carbon SH800, which has by far the highest amount of pores with widths >1.5 nm. The incipient mesopore network in material SH800 is compensated by a very high volume of larger micropores ($V_{\alpha\ super}$). The micropores distribution in the commercial material and its well-developed mesopore structure, allows the
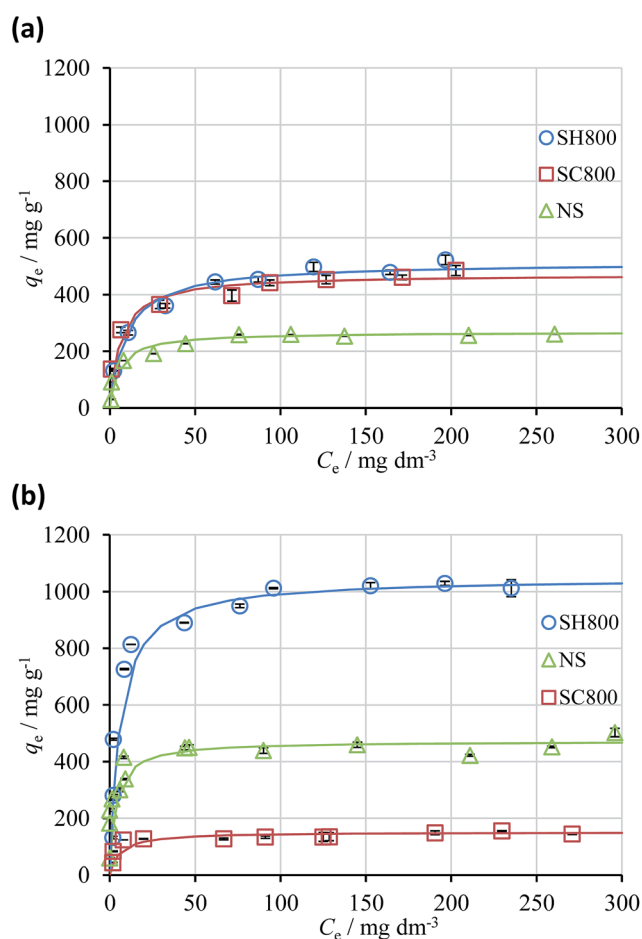

(a)

(b)

Fig. 7 Paracetamol (a) and iopamidol (b) adsorption isotherms on the studied carbons at 30 °C. Symbols correspond to the experimental data, whereas lines represent the fitting to the Langmuir equation. Error bars are included.

adsorption of all the iopamidol species; however, the total volume of pores available is still considerably lower than that of carbon SH800.

3.2.3 Paracetamol and iopamidol equilibrium adsorption studies.

The equilibrium adsorption isotherms are displayed in Fig. 7. In all the systems, the curves are characterized by a steep initial rise that approaches a plateau attributed to the formation of a complete monolayer and belong to the L-type.[45,46] The experimental data were fitted to the linear forms of the Langmuir[26] and Freundlich[27] equations quoted in Table S1,† and the fitting parameters, the determination coefficients and chi-square test analysis values are presented in Table 5.

In the case of paracetamol (Fig. 7(a)), both lab-made materials have very similar curves and outperform the commercial activated carbon, reaching almost the double of the adsorption capacity. From the isotherms obtained for iopamidol, (Fig. 7(b)) the lab-made carbon SH800 stands out with a remarkably high adsorption capacity, whereas the carbon SC800 has the lowest adsorption capacity.

The values of determination coefficient (R^2) and of the non-linear chi-square analysis (χ^2) indicate a better adjustment of the experimental data to the Langmuir model. The monolayer adsorption capacities (q_m) calculated from the model are in accordance with the analysis of the isotherms. The values of the Langmuir constant (K_L) are similar in all the cases, indicating the identical affinity of the two pharmaceutical compounds for the carbons assayed.

The values of the monolayer adsorption capacities are usually presented in mg of adsorbate per gram of adsorbent; however, when species with very distinct molecular weights are involved, as is the case of paracetamol and iopamidol, the comparison of the adsorption capacities must be made in mmol of adsorbate per gram of adsorbent. In fact, although carbon SH800 presents a remarkably high adsorption capacity for iopamidol when expressed in mg g^{-1}, when the values are expressed in mmol g^{-1}, it is clearly seen that the number of paracetamol structural units adsorbed onto carbon SH800 is more than the double of the iopamidol (*i.e.* 3.4 *versus* 1.4 mmol

g^{-1}, respectively). This is the expected behavior, because smaller species allow the optimization of the porous volume occupied. The lower number of iopamidol moles adsorbed compared with paracetamol is also in line with its higher solubility (Table 3). For carbon SC800 q_m(Para) $\approx$ 16 $\times$ q_m(Iop) in mmol g^{-1} which is understood considering the absence of micropores wide enough to adsorb the iopamidol bigger aggregates. The presence of a high number of micropores with apertures between 0.5 and 1.3 nm that allows the diffusion and adsorption of the paracetamol monomer or dimer.

The values gathered in Table 6 show that the sucrose-derived activated carbons assayed in this study for the adsorption of paracetamol and iopamidol outperform those of commercial and waste-derived activated carbons tested in similar experimental conditions, highlighting the potentialities of these sustainable materials to be used in water treatment technologies to remove organic compounds.

If the adsorption capacity is the only parameter taken into account to select an adsorbent for decontamination purposes, material SH800 would be elected. However, the preparation yield of this material is considerably lower than that of material SC800, which, in the case of paracetamol, has a similar performance. Thus, the use of mixtures of these two materials, preferably with a higher percentage of carbon SC800, could be an option to ensure high removal efficiencies of the organic compounds of different molecular weight. Moreover, carbon SC800 has a microspherical morphology, which gives it a considerably higher tap and packing densities than those of material SH800,[10] and this a crucial property for the storage and handling of these powdered materials. On the other hand, concerning the water purification purposes, the study developed by Ellerie *et al.*[48] highlights the importance of the particle size in activated carbons used as adsorptive coating materials for microfiltration, because activated carbons constituted by submicron-sized and micron-sized particles (as is the case of K_2CO_3-activated hydrochars obtained in this study) can potentially serve as effective secondary membranes, preventing foulants such as organic

Table 5 Fitting parameters to the Langmuir and Freundlich models and chi-square test analysis, χ^2. Langmuir parameters: q_m – monolayer adsorption capacity, K_L – Langmuir constant. Freundlich parameters: n_F – Freundlich exponent, K_F – Freundlich constant

	Langmuir equation					Freundlich equation			
	q_m (mg g^{-1})	$q_m{}^a$ (mmol g^{-1})	K_L (dm^3 mg^{-1})	R^2	χ^{2b}	$1/n$	K_F (mg$^{1-1/n}$ (dm^3)$^{1/n}$ g^{-1})	R^2	χ^{2b}
Paracetamol									
SH800	513.5	3.397	0.105	0.997	7.0	0.308	115.1	0.960	24.3
SC800	471.8	3.121	0.157	0.997	12.7	0.227	155.4	0.952	15.2
NS	267.7	1.771	0.180	0.997	5.3	0.350	56.4	0.862	47.0
Iopamidol									
SH800	1049.6	1.351	0.173	0.999	33.3	0.285	261.5	0.706	360.1
SC800	150.9	0.194	0.174	0.996	19.5	0.163	64.1	0.711	19.7
NS	472.4	0.608	0.284	0.992	30.2	0.097	282.7	0.755	33.9

^{a} Calculated considering the molecular weight of a paracetamol or iopamidol monomer. ^{b} $\chi^2 = \sum \dfrac{(q_e - q_{e,m})^2}{q_{e,m}}$ where q_e is the experimental equilibrium uptake and $q_{e,m}$ is the equilibrium uptake calculated from the model.[47]

Table 6 Maximum adsorption capacity values of several activated carbons for paracetamol and iopamidol in similar experimental conditions (*i.e.* temperature, range of concentration of PhAC, agitation speed). The maximum adsorption capacity for each PhAC is highlighted in bold

| | Adsorption capacity | | |
Adsorbent	(mg g^{-1})	(mmol g^{-1})^a	Ref.
Paracetamol			
Commercial activated carbon	255	1.687	49
Cork-derived activated carbon	200	1.323	49
Peach stone-derived activated carbon	204	1.350	49
Plastic-derived activated carbon	113	0.748	49
Pine fly ash-derived activated carbons	189–244	1.250–1.614	11
Commercial activated carbon	170	1.125	11
Pine char-derived activated carbons	270 and 434	1.786 and 2.871	19
Sucrose-derived activated carbons	472 and **514**	3.123 and **3.401**	Present work
Commercial activated carbon	267	1.766	Present work
Iopamidol			
Commercial activated carbons	136 and 147	0.175 and 0.189	18
Sisal-derived activated carbons	105 and 112	0.135 and 0.144	18
Sucrose-derived activated carbons	151 and **1050**	0.194 and **1.351**	Present work
Commercial activated carbon	472	0.607	Present work

^{a} Calculated considering the molecular weight of a paracetamol or iopamidol monomer.

matter from reaching the microfiltration or ultrafiltration membrane without greatly restricting the flow.

4. Conclusions

The two-step methodology involving the HTC of renewable biomass (*i.e.* sucrose) and further chemical activation allowed obtaining activated carbons with remarkably high adsorption capacities for pharmaceutical compounds, when compared with commercial materials or other lignocellulosic-derived activated carbons.

The sucrose-derived activated carbons obtained are microporous solids with distinct morphologies and micropore size distributions. KOH activation leads to superactivated carbons (up to 2400 m^2 g^{-1}) presenting wide micropore size distributions and sponge-like morphologies. Carbons prepared with K$_2$CO$_3$ as activating agent retain the spherical shape of the hydrochar, attain apparent surface areas around ~1400 m^2 g^{-1} and present narrow micropore size distributions centered in the ultramicropore region.

The high adsorption capacities of the KOH activated materials for all the pharmaceutical compounds assayed are related to their high number of larger micropores. The materials obtained by K$_2$CO$_3$ activation have similar capacity for the adsorption of the small pharmaceuticals, but lower removal efficiency for the bulkier compound, iopamidol, due to the absence of micropores to accommodate the iopamidol trimer.

K$_2$CO$_3$ activation of hydrochars is a promising methodology to prepare micrometer-sized activated carbons, which can present great advantages to be used as filter media alone or coupled to membrane systems in water purification technologies. In this sense, the present work constitutes an important contribution towards the search for the best available materials for water treatment processes in order to face the problems of water streams' contamination with pharmaceutical compounds, which is receiving increasing attention from both scientific and governmental entities.

Acknowledgements

References

1 A. P. Carvalho, A. S. Mestre, M. Andrade and C. O. Ania, in *Ibuprofen: Clinical pharmacology, medical uses and adverse effects*, ed. W. C. Carter and B. R. Brown, Nova Science Publishers, 2013, ch. 1, pp. 1–84.

2 A. P. Carvalho, A. S. Mestre, M. Haro and C. O. Ania, in *Acetaminophen: Properties, clinical uses and adverse effects*, ed. A. Javaherian and P. Latifpour, Nova Science Publishers, 2012, ch. 4, pp. 57–105.

3 POSEIDON, *Assessment of technologies for the removal of pharmaceuticals and personal care products in sewage and drinking water facilities to improve the indirect potable water reuse, Final Report*, June 2004.

4 M.-M. Titirici, R. J. White, C. Falco and M. Sevilla, *Energy Environ. Sci.*, 2012, **5**, 6796–6822.

5 M.-M. Titirici, in *Novel Carbon Adsorbents*, ed. J. M. D. Tascón, Elsevier, Amsterdam, 2012, ch. 12, pp. 351–399.

6 C. Falco, J. P. Marco-Lozar, D. Salinas-Torres, E. Morallón, D. Cazorla-Amorós, M. M. Titirici and D. Lozano-Castelló, *Carbon*, 2013, **62**, 346–355.

7 M. Sevilla, A. B. Fuertes and R. Mokaya, *Energy Environ. Sci.*, 2011, **4**, 1400–1410.

8 A. J. Romero-Anaya, M. Ouzzine, M. A. Lillo-Ródenas and A. Linares-Solano, *Carbon*, 2014, **68**, 296–307.

9 C. L. He, Y. L. Liu, Z. P. Xue, M. T. Zheng, H. B. Wang, Y. Xiao, H. W. Dong, H. R. Zhang and B. F. Lei, *Int. J. Electrochem. Sci.*, 2013, **8**, 7088–7098.

10 A. S. Mestre, C. Freire, J. Pires, A. P. Carvalho and M. L. Pinto, *J. Mater. Chem. A*, 2014, **2**, 15337–15344.

11 M. Galhetas, A. S. Mestre, M. L. Pinto, I. Gulyurtlu, H. Lopes and A. P. Carvalho, *Chem. Eng. J.*, 2014, **240**, 344–351.

12 A. S. Mestre, A. S. Bexiga, M. Proença, M. Andrade, M. L. Pinto, I. Matos, I. M. Fonseca and A. P. Carvalho, *Bioresour. Technol.*, 2011, **102**, 8253–8260.

13 A. S. Mestre, S. C. R. Marques and A. P. Carvalho, *Ind. Eng. Chem. Res.*, 2012, **51**, 9850–9857.

14 A. S. Mestre, M. L. Pinto, J. Pires, J. M. F. Nogueira and A. P. Carvalho, *Carbon*, 2010, **48**, 972–980.

15 A. S. Mestre, J. Pires, J. M. F. Nogueira and A. P. Carvalho, *Carbon*, 2007, **45**, 1979–1988.

16 A. S. Mestre, J. Pires, J. M. F. Nogueira, J. B. Parra, A. P. Carvalho and C. O. Ania, *Bioresour. Technol.*, 2009, **100**, 1720–1726.

17 A. S. Mestre, R. A. Pires, I. Aroso, E. M. Fernandes, M. L. Pinto, R. L. Reis, M. A. Andrade, J. Pires, S. P. Silva and A. P. Carvalho, *Chem. Eng. J.*, 2014, **253**, 408–417.

18 A. S. Mestre, M. Machuqueiro, M. Silva, R. Freire, I. M. Fonseca, M. S. C. S. Santos, M. J. Calhorda and A. P. Carvalho, *Carbon*, 2014, **77**, 607–615.

19 M. Galhetas, A. S. Mestre, M. L. Pinto, I. Gulyurtlu, H. Lopes and A. P. Carvalho, *J. Colloid Interface Sci.*, 2014, **433**, 94–103.

20 S. J. Gregg and K. S. W. Sing, *Adsorption, Surface Area and Porosity*, Academic Press Inc., London, 1982.

21 L. Gurvich, *J. Soc. Phys.-Chim. Russe*, 1915, **47**, 805–827.

22 F. Rodríguez-Reinoso, J. M. Martin-Martinez, C. Prado-Burguete and B. McEnaney, *J. Phys. Chem.*, 1987, **91**, 515–516.

23 M. L. Pinto, A. S. Mestre, A. P. Carvalho and J. Pires, *Ind. Eng. Chem. Res.*, 2010, **49**, 4726–4730.

24 J. S. Noh and J. A. Schwarz, *J. Colloid Interface Sci.*, 1989, **130**, 157–164.

25 Y.-S. Ho, *J. Hazard. Mater.*, 2006, **136**, 681–689.

26 I. Langmuir, *J. Am. Chem. Soc.*, 1918, **40**, 1361–1403.

27 H. M. F. Freundlich, *J. Phys. Chem.*, 1906, **57**, 385–470.

28 M. Sevilla and A. B. Fuertes, *Energy Environ. Sci.*, 2011, **4**, 1765–1771.

29 J. Wang and S. Kaskel, *J. Mater. Chem.*, 2012, **22**, 23710–23725.

30 D. Lozano-Castello, J. M. Calo, D. Cazorla-Amoros and A. Linares-Solano, *Carbon*, 2007, **45**, 2529–2536.

31 E. Raymundo-Pinero, P. Azais, T. Cacciaguerra, D. Cazorla-Amoros, A. Linares-Solano and F. Beguin, *Carbon*, 2005, **43**, 786–795.

32 B. Cardoso, A. S. Mestre, A. P. Carvalho and J. Pires, *Ind. Eng. Chem. Res.*, 2008, **47**, 5841–5846.

33 L. Wei, M. Sevilla, A. B. Fuertes, R. Mokaya and G. Yushin, *Adv. Energy Mater.*, 2011, **1**, 356–361.

34 M. Sevilla and R. Mokaya, *Energy Environ. Sci.*, 2014, **7**, 1250–1280.

35 D. Nematollahi, H. Shayani-Jam, M. Alimoradi and S. Niroomand, *Electrochim. Acta*, 2009, **54**, 7407–7415.

36 M. M. Miller, S. P. Wasik, G. L. Huang, W. Y. Shiu and D. Mackay, *Environ. Sci. Technol.*, 1985, **19**, 522–529.

37 M. E. Essington, *Soil and water chemistry: An integrative approach*, CRC Press, Boca Raton, 2004.

38 T. A. Ternes, M. Bonerz, N. Herrmann, B. Teiser and H. R. Andersen, *Chemosphere*, 2007, **66**, 894–904.

39 S. W. Nam, D. J. Choi, S. K. Kim, N. Her and K. D. Zoh, *J. Hazard. Mater.*, 2014, **270**, 144–152.

40 R. A. Granberg and Å. C. Rasmuson, *J. Chem. Eng. Data*, 1999, **44**, 1391–1395.

41 O. Lorphensri, D. A. Sabatini, T. C. G. Kibbey, K. Osathaphan and C. Saiwan, *Water Res.*, 2007, **41**, 2180–2188.

42 A. Nabiço, P. L. Figueiredo, I. M. Fonseca, A. P. Carvalho and A. S. Mestre, *Clofibric acid adsorption process onto carbons: effect of pH and water hardness*, Extended Abstracts of the XII Reunión del Grupo Español del Carbón (Oral presentation), Madrid (Spain), 2013.

43 E. Fklder, M. Grandi, D. Pitre and G. Vittadini, *Analytical Profiles of Drug Substances*, Academic Press, 1988.

44 Y. S. Ho and G. McKay, *Process Biochem.*, 1999, **34**, 451–465.

45 R. Denoyel, F. Rouquerol and J. Rouquerol, in *Adsorption by Carbons*, ed. E. J. Bottani and J. M. D. Tascón, Elsevier Ltd, Oxford, 2008, ch. 12, pp. 273–300.

46 R. Denoyel and F. Rouquerol, in *Handbook of Porous Solids*, ed. F. Schüth, K. S. W. Sing and J. Weitkamp, Wiley-VCH, Weinheim, 2002, vol. 1, ch. 2.6, pp. 276–308.

47 Y.-S. Ho, *Carbon*, 2004, **42**, 2115–2116.

48 J. R. Ellerie, O. G. Apul, T. Karanfil and D. A. Ladner, *J. Hazard. Mater.*, 2013, **261**, 91–98.

49 I. Cabrita, B. Ruiz, A. S. Mestre, I. M. Fonseca, A. P. Carvalho and C. O. Ania, *Chem. Eng. J.*, 2010, **163**, 249–255.